

Numerical Analysis on the Performance of Heatsink with Microchannels

Jer-Huan Jang, Han-Chieh Chiu, Wei-Chung Yeih, Jia-Jui Yang, Chien-Sheng Huang

Abstract—In this paper, numerical simulation is used to investigate the thermal performance of liquid cooling heatsink with microchannels due to geometric arrangement. Commercial software ICEPAK is utilized for the analysis. The considered parameters include aspect ratio, porosity and the length and height of microchannel. The aspect ratio varies from 3 to 16 and the length of microchannel is 10mm, 14mm, and 18mm. The height of microchannel is 2mm, 3mm and 4mm. It is found short channel have better thermal efficiency than long channel at 490Pa. No matter the length of channel the best aspect ratio is 4. It is also noted that pressure difference at 2940Pa the best aspect ratio from 4 to 8, it means pressure difference affect aspect ratio, effective thermal resistance at low pressure difference but lower effective thermal resistance at high pressure difference.

Keywords—thermal resistance, liquid cooling, microchannels, numerical analysis, pressure difference

I. INTRODUCTION

As the electronics technology develops into microscale, electronic devices have been fabricated with compact size and higher power. This trend leads to higher power densities and more stringent temperature constraints in electronic devices. The conventional cooling methods can no longer meet the highly demanding cooling requirement. The heat removal problem has become an important factor in the advancement of microelectronics.

The microchannel heat sink, introduced by Tuckermann and Pease [1] is one of the ingenious ways of improving the heat removal rate effectively. They first recognized the potential of microchannel heat sink and demonstrated that electronics chips could be effectively cooled by means of forced convection flow of water through the microchannels.

J. H. Jang is with the Graduate Institute of Electro-Mechanical Engineering of Ming Chi University of Technology, Taishan, New Taipei City, Taiwan 24301 (phone: 886-2-29089899 ext. 4522; fax: 886-2-29063269; e-mail: jhjjang@mail.mcut.edu.tw)

H. C. Chiu is with the Department of Mechanical Engineering of Technology and Science Institute of Northern Taiwan, Peitou, Taipei, Taiwan 11201 (e-mail: hcchiu@tsint.edu.tw)

W.C. Yeih is with the Department of Harbor and River Engineering of National Taiwan Ocean University, Keelung, Taiwan 202 (e-mail: wcyeih@mlab.hre.ntou.edu.tw)

J.J. Yang is a graduate student with the Graduate Institute of Electro-Mechanical Engineering of Ming Chi University of Technology, Taishan, New Taipei City, Taiwan 24301 (e-mail: gn01678153@yahoo.com.tw)

C.S. Huang is a graduate student with the Graduate Institute of Electro-Mechanical Engineering of Ming Chi University of Technology, Taishan, New Taipei City, Taiwan 24301 (e-mail: z75102595@hotmail.com)

Afterwards, microchannels have been one of the potential solutions for the enhancement of heat transfer. Peng *et al.* [2-4] studied the influence of geometry on heat transfer performance of rectangular microchannels. According to their results [4], there was an optimal geometry design under fixed height and total cross section area. Qu *et al.* [5] studied heat transfer of micro rectangular and trapezoidal channels in silicon wafers. Rahman [6] investigated heat transfer performance of parallel and serpentine microchannels in silicon wafers. Kim and Mudawar [7], [8], Gunnasegaran *et al.* [9], Chen *et al.* [10], McHale and Garimella [11] investigated fluid flow and heat transfer characteristics of different shapes microchannel heat sink which are rectangular, trapezoidal, triangular, inverse trapezoidal, diamond-shaped and circular.

In recent years, more works [12] – [15] have been dedicated to studied heat transfer of microchannels with CFD. Kuo *et al.* [12] assessed effect of channel geometry on heat transfer of fully developed flow. They found the optimal channel width decreased with increasing pumping power. Foli *et al.* [13] explored optimal cross section geometry based on constant cross section area. The pressure gradient was found to be linear with respect to aspect ratio. Li and Peterson [14] studied channel design with CFD. The corresponding aspect ratio and porosity for optimal condition were 12 and 60%, respectively. Chen [15] considered the effect of inertia and investigated the whole performance of microchannel array.

Other works investigated optimal geometrical conditions of channels. Knight *et al.* [16] approximately approached the solution with fin concept. The temperature on the channel cross section was considered uniform. Kim and Kim [17] utilized the concept of porous material to analyze microchannels. In that concept, the volumetric parameter and two-equation model were employed to solve the thermal fluid field. The flow field was considered as a porous material with mixed solid and liquid. There should be an extra equation to describe the heat transfer between the solid and the liquid. Zhao and Lu [18] explored the heat transfer of microchannels with the same concept. In their study, the channel geometry was specified by cross section porosity and aspect ratio. Lee *et al.* [19] studied heat transfer of various channels with different widths and constant aspect ratio 5.0.

In previous literatures, some researchers use Reynolds number larger than 5000 to achieve an equivalent thermal resistance below 0.1°C/W, however, the driving pressure would be several atmosphere.

Actually, this operation condition is not realistic in ordinary electronic cooling system. The driving pressure within microchannels should be less than 5000Pa. In addition, the analysis in some studies only use single microchannel as the computational domain. This is questionable for a heatsink with microchannels. Also, the material of heatsink with aluminum is not under investigation.

Motivated by the literatures cited above, the purpose of present study is to investigate the thermal performance of heatsink with microchannels under space limit condition with the same pressure and flow rate. Numerical analysis is carried out to simulation the model with geometric parameters, such as microchannel height, porosity, and aspect ratio. Two driving pressure difference is applied to the model for simulation

II. GEOMETRIC MODEL

The microchannel heatsink used in this research is schematically described in Fig. 1. The heatsink is made of aluminum. Due to specific application, the model is the total thickness of the heatsink is limited to 4.0mm. The microchannel height is set to be 2mm with 1mm thickness for top and bottom plate. The main section of the heatsink covers an area of 20.0mm x 14.0mm, including an area of 10.0mm x 10.0mm occupied by the microchannel block. The lengthened inlet and outlet is designed to obtain a fully developed flow for both inlet and outlet. The heat source area is 10mm x 10mm attached to the bottom surface of the heatsink.

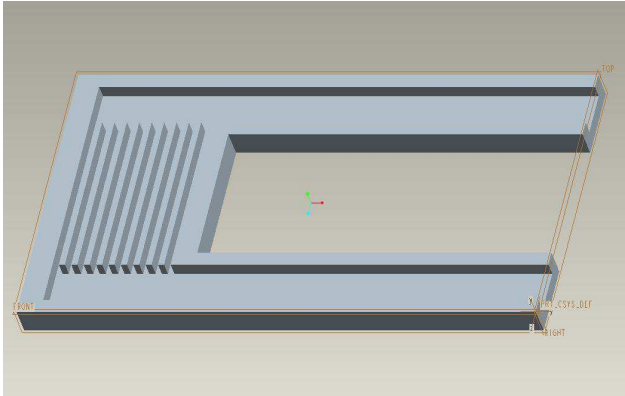


Fig. 1 profile within the heatsink

The buffer zone is to unify the flow velocity for each microchannel such that a better heat transfer performance is obtained. In fact, the flow velocity for each microchannel is not identical, the inlet and outlet arrangement will effect on the heat transfer of the heatsink. Result of effect on the inlet and outlet arrange will be discussed in the later section.

Porosity of heatsink with microchannels is calculated as the ratio of total microchannel width to the summation of total microchannel width and total fin thickness. The aspect ratio is defined as the ratio of microchannel height to microchannel width.

III. NUMERICAL ANALYSIS

A commercial code ICEPAK was employed to simulate the

three dimensional thermal and flow fields. The temperature field for solid region was solved with energy equation. The flow field was considered as steady, laminar and incompressible under low driving pressure conditions. The governing equations for the flow field are continuity equation, momentum equations in three directions (x, y, and z), and energy equation as follow:

$$\frac{\partial u}{\partial x} + \frac{\partial v}{\partial y} + \frac{\partial w}{\partial z} = 0 \quad (1)$$

$$\frac{\partial P}{\partial x} = \mu \left(\frac{\partial^2 u}{\partial x^2} + \frac{\partial^2 u}{\partial y^2} + \frac{\partial^2 u}{\partial z^2} \right) \quad (2)$$

$$\frac{\partial P}{\partial y} = \mu \left(\frac{\partial^2 v}{\partial x^2} + \frac{\partial^2 v}{\partial y^2} + \frac{\partial^2 v}{\partial z^2} \right) \quad (3)$$

$$\frac{\partial P}{\partial z} = \mu \left(\frac{\partial^2 w}{\partial x^2} + \frac{\partial^2 w}{\partial y^2} + \frac{\partial^2 w}{\partial z^2} \right) \quad (4)$$

$$u \frac{\partial T}{\partial x} + v \frac{\partial T}{\partial y} + w \frac{\partial T}{\partial z} = \frac{k_i}{\rho c_p} \left(\frac{\partial^2 T}{\partial x^2} + \frac{\partial^2 T}{\partial y^2} + \frac{\partial^2 T}{\partial z^2} \right) \quad (5)$$

where u , v , and w are velocities in x, y, z directions, respectively. T denotes temperature, k_i , c_p , and ρ are thermal conductivity, specific heat, and density of liquid, respectively.

For simplicity, the cross sections of the inlet and the outlet of heatsink were modified to rectangular shape with the same cross sectional area as original circular one. The pressure difference between the inlet and the outlet is given by the water level difference of the experiment. The flow velocity on all solid walls were set zero. The outer solid walls were set to be adiabatic. The error due to this assumption is ignorable compared with the heat transferred through convection from water flow. Structural grids were generated to solve this problem. Grids near the boundary walls were set denser to obtained accurate results. Basically, each solid region at least is divided into 5 elements; while fluid segment is divided into 8 grids. The total grid is approximately 300,000~1,500,000 nodes. In the calculation, the convergence criteria between two consecutive iterations is set to be relative deviation less than 1×10^{-3} for velocity and continuity, and less than 1×10^{-6} for solution in energy equation.

The effective thermal resistance, which is an index for heat transfer performance of heatsink, can be defined as

$$R_{th} = \frac{T_{max} - T_{in}}{\dot{Q}} \quad (6)$$

where T_{max} is the maximum temperature, T_{in} is the inlet water temperature, and \dot{Q} is the heating power with unit of watt.

IV. RESULTS AND DISCUSSION

In the model, two applying pressure differences, 490Pa and 2940Pa, are applied for driving the flow. The working fluid is water with inlet temperature of 25°C. The applied heating power is 21W, such that the power density is 210,000W/m².

The numerical model is compared with the experimental result of Chiu *et al.* [20] for verification, and it shows in good agreement.

Detailed experimental procedure and numerical simulation are presented in [20]. Fig. 2 shows the velocity and temperature

contour diagram of the model with 53% porosity, AR= 3.77 (microchannel width=0.53mm), microchannel length=10mm, and the applying pressure difference=490Pa. It is observed that the flow velocity is the largest at the inlet and outlet with parabolic profile in Fig. 2(a). The velocity in the microchannels on the lower side of the figure is little less than that at the center. It is also found that the temperature increases as the flow to the downstream in Fig. 2(b). The highest temperature is close to the 1/4 channel length at the downstream. The peak temperature has been shifted towards to the top of the figure. Apparently, the peak temperature is shifted due to the flow speed is higher for the top microchannels. However, for higher applying pressure difference, the temperature contour shows symmetric pattern due to higher flow speed at the lower part of the microchannels. In other cases for present study is not shown due to limitation of this paper.

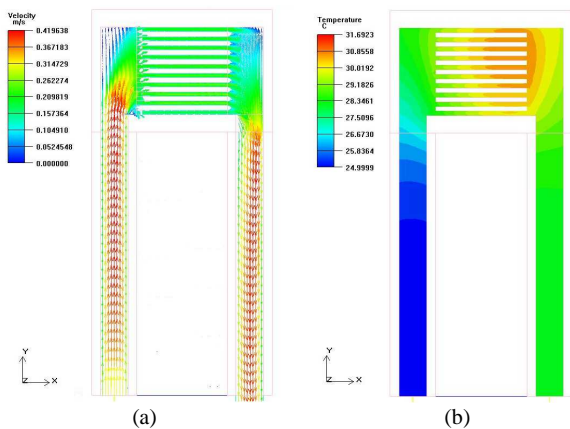


Fig. 2 (a)velocity; and (b) temperature contour diagram of the model

A. Effect of microchannel length

The microchannel length effects on the heat transfer of the heatsink. The microchannel length is set 10mm, 14mm, and 18mm to investigate this effect with high (2940Pa) and low (490Pa) applying pressure difference. The porosity is set to be 53%. Effect of microchannel length is depicted in Fig. 3. It is obvious that the thermal resistance increases as microchannel length increases. This is because higher temperature difference in the upstream of microchannel, resulting higher heat transfer. The thermal resistance shows an optimal value with high applying pressure difference at a given AR value.

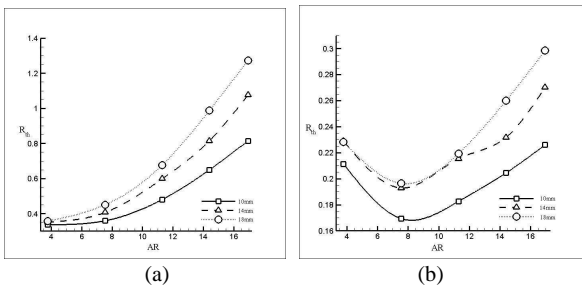


Fig. 3 Effect of microchannel length with applying pressure difference (a) 490Pa; and (b) 2940Pa

B. Effect of porosity

Fig. 4 presents the effect of porosity on the thermal resistance of heatsink with low and high applying pressure differences. It is seen that the thermal performance decreases as porosity increases for low applying pressure difference (490Pa) in Fig. 4(a). At low applying pressure difference, the thermal performance is about the same with 53% and 75% of porosity, which means the porosity is not necessary to be high for low applying pressure difference. However, the thermal resistance values are high when AR is large. The may be due to high pressure lost with high AR and low applying pressure difference. In Fig. 4(b), it is observed that the heat transfer with 53% is the best among the three cases at a given AR value for high applying pressure difference. It means an optimum porosity value exists for a given aspect value. In addition, comparing two figures in Fig. 4, it also shows that the applying pressure difference influence on the thermal performance.

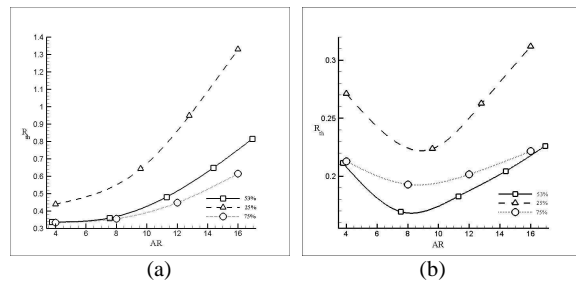


Fig. 4 Effect of porosity applying pressure (a) 490Pa; and (b) 2940Pa

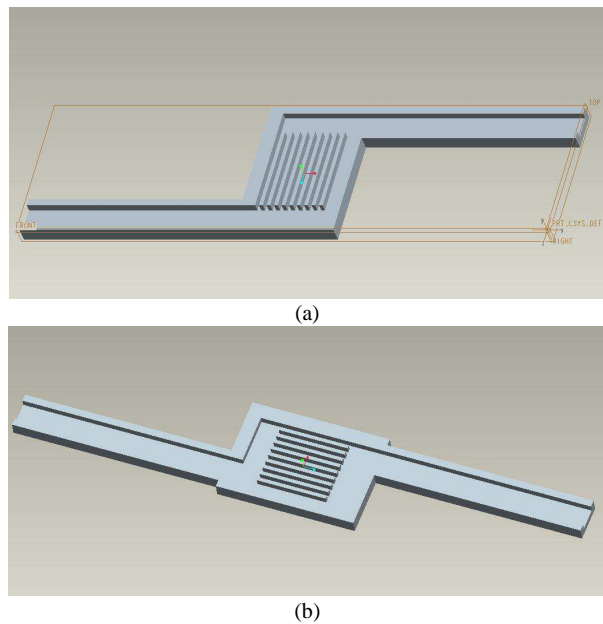


Fig. 5 Entrance arrangement configuration: (a) Type-2;(b)Type-3

C. Entrance effect

As mentioned previously, the arrangements of inlet and outlet are discussed in this section. The arrangement of Fig. 1 is called Type-1 arrangement. Fig. 5 shows the Type-2 and Type-3 arrangements. In some researches, Type-1, Type-2, and Type-3

design are called the U-type, N-type, and Z-type design. Entrance effect is presented in Fig. 6. In all three cases, the porosity is set at 53%, microchannel length is 10mm. For low applying pressure difference, all the three arrangements show little difference on the thermal performance, while a large thermal performance difference for high applying pressure difference. Due to a large pressure loss for porosity of 53% with low applying pressure difference, the entrance effect is not insignificant. As shown in Fig. 6(b), the best arrangement among the three is Type-1. It is also noticed that the optimal AR varies with the entrance arrangement. The optimal value varies from 8 to 9.

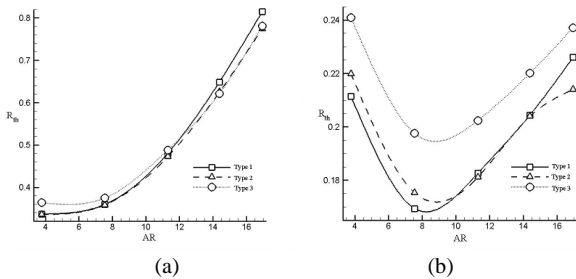


Fig. 6 Entrance effect with applying pressure difference (a) 490Pa; and (b) 2940Pa

D. Effect of microchannel height

Microchannel Geometry effects on the thermal performance of heatsink with microchannels. The microchannel height effect is also investigated. Due to limitation of the height of heatsink for specific application, only 3mm and 4mm microchannel height are study. Fig. 7 shows effect of microchannel heights of 3mm and 4mm for high applying pressure difference. It is found that the microchannel length effect is the same as previous discussion with different microchannel height. It is also found that the thermal resistance decreases as microchannel height increases by comparing Fig. 3(b) and Fig. 7. This is because more water flow into the heatsink with a given applying pressure difference.

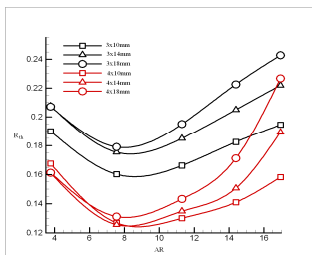


Fig. 7 Effect of microchannel length with high applying pressure difference (2940Pa) for 3mm and 4mm microchannel height

E. Effect of multilayer design

Vafai and Zhu [21] proposed a new concept for a two-layered microchannel heatsink for cooling of the electronic components. They found that the pressure drop required for the two-layered heatsink was found to be substantially smaller than that of the one-layered heatsink. In this paper, a two-layered heatsink with microchannels has been compared with two-layered heatsink with microchannels. Fig. 8 shows the configuration of the

two-layer heat sink with microchannels. Between the two layers is 1mm thickness of plate.

The flow direction of upper and lower layer microchannels is the same.

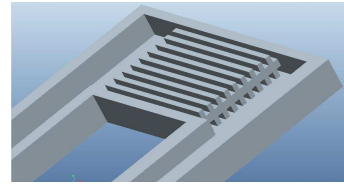


Fig. 8 profile within the heatsink

Fig. 9 presents the comparison of heatsink with 3mm microchannel height and heatsink with two-layer microchannels. The microchannel height of heatsink with two-layer microchannels is 1mm for each layer, such that the total height of the heatsink would be the same. It is observed that the thermal resistance of two-layer heatsink design is higher than that of 3mm microchannel height for both high and low applying pressure differences. Apparently, the flow resistance is higher and more water is flowing through for heatsink with single layer microchannels, in turns the thermal resistance is lower for heatsink with single layer microchannels.

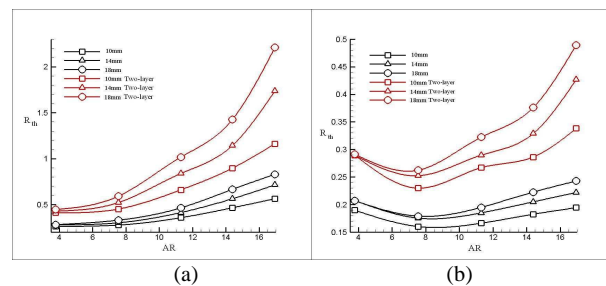


Fig. 9 Effect of microchannel length for 3mm microchannel height and two-layer with (a) 490 Pa and (b) 2940Pa

V. CONCLUSIONS

Based on the numerical analysis in heatsink with microchannels, several concluding remarks are drawn as follow:

1. Under same applying pressure difference, the thermal resistance increases as microchannel length increases.
2. The thermal resistance shows an optimal value with different applying pressure difference at a given AR value. The corresponding aspect ratio for the lowest effective resistance is dependent on applying pressure difference of heatsink with microchannels.
3. With high applying pressure difference, thermal performance of porosity=53% is the best among 25%, 53% and 75% porosity.
4. The heat transfer enhancement due to increase applying pressure difference is more significant on microchannels with high aspect ratio. Hence thinner channels are more advantageous under high pressure gradient.
5. The thermal resistance decreases as microchannel height increase. This is because more water flow into the heatsink with a given pressure difference.

ACKNOWLEDGMENTS

The financial support of this research by the National Science Council, Taiwan, under the Contract NSC100-2221-E-131-035, is appreciated. Also, the support from Technology and Science Institute of Northern Taiwan is acknowledged.

REFERENCES

- [1] D.B. Tuckermann and R.F.W. Pease, High performance heat sinking for VLSI, *IEEE Electronic Device Lett.* EDL-2, pp.126-129, 1981.
- [2] X.F. Peng, B.X. Wang, G.P. Peterson, and H.B. Ma, Experimental investigation of heat transfer in flat plates with rectangular microchannels, *Int. J. Heat Mass Transfer*, 38, pp. 127-137, 1995.
- [3] X.F. Peng and G.P. Peterson, Friction flow characteristics of water flowing through rectangular microchannels, *J. Exp. Heat Transfer*, 7, pp. 249-264, 1995.
- [4] X.F. Peng and G.P. Peterson, Convective heat transfer and flow friction for water flow in microchannel structures, *Int. J. Heat Mass Transfer*, 39, pp. 2599-2608, 1996.
- [5] W. Qu, G. M. Mala, and D. Li, Heat transfer for water flow in trapezoidal silicon microchannels, *Int. J. Heat Mass Transfer*, 43, pp. 3925-3936, 2000.
- [6] M.M. Rahman, Measurements of heat transfer in microchannel heat sink, *Int. Comm. Heat Mass Transfer*, 27, pp. 495-506, 2000.
- [7] S. M. Kim and I. Mudawar, Analytical heat diffusion models for different micro-channel heat sink cross-sectional geometries, *Int. J. Heat Mass Transfer*, 53, pp. 4002-4016, 2010.
- [8] S. M. Kim and I. Mudawar, Analytical heat diffusion models for heat sinks with circular micro-channels, *Int. J. Heat Mass Transfer*, 53, pp. 4552-4566, 2010.
- [9] P. Gunnasegaran, H. A. Mohammed, N. H. Shuaib, and R. Saidur, The effect of geometrical parameters on heat transfer characteristics of microchannels heat sink with different shapes, *Int. Comm. Heat Mass Transfer*, 37, pp. 1078-1086, 2010.
- [10] Y. Chen, C. Zhang, M. Shi, and J. Wu, Three-dimensional numerical simulation of heat and fluid flow in noncircular microchannel heat sinks, *Int. Comm. Heat Mass Transfer*, 36, pp. 917-920, 2009.
- [11] J. P. McHale, and S. V. Garimella, Heat transfer in trapezoidal microchannels of various aspect ratios, *Int. J. Heat Mass Transfer*, 53, pp. 365-375, 2010.
- [12] H.S. Kou, J.J. Lee, and C.W. Chen, Optimal thermal performance of microchannel heatsink by adjusting channel width and height, *Int. Comm. Heat Mass Transfer*, 35, pp. 577-582, 2008.
- [13] K. Foli, T. Okabe, M. Olhofer, Yaochu Jin, and B. Sendhoff, Optimization of the micro heat exchanger: CFD, analytical approach and multi-objective evolutionary algorithms, *Int. J. Heat Mass Transfer* 49, pp. 1090-1099, 2005.
- [14] J. Li and G.P. Peterson, 3-Dimensional numerical optimization of silicon-based high performance parallel microchannel heatsink with liquid flow, *Int. J. Heat Mass Transfer*, 50, pp. 2895-2904, 2007.
- [15] C.H. Chen, Forced convection heat transfer in microchannel heatsinks, *Int. J. Heat Mass Transfer*, 50, pp. 2182-2189, 2007.
- [16] R.W. Knight, J.S. Goodling and D. J. Hall, Optimal thermal design of forced convection heatsinks---Analytical, *ASME J. Electron. Packag.*, 113, pp. 313-321, 1986.
- [17] S.J. Kim and D. Kim, Forced convection in microstructures for electronic equipment cooling, *ASME J. Heat Transfer*, 121, pp. 635-645, 1999.
- [18] C.Y. Zhao and T.J. Lu, Analysis of microchannel heatsinks for electronics cooling, *Int. J. Heat Mass Transfer*, 45, pp. 4857-4869, 2002.
- [19] P.S. Lee, S.V. Garimella, and D. Liu, Investigation of heat transfer in rectangular microchannels, *Int. J. Heat Mass Transfer*, 48, pp. 1688-1704, 2005.
- [20] H.C. Chiu, J.H. Jang, H.W. Yeh, and M.S. Wu, The heat transfer characteristics of liquid cooling heatsink containing microchannels, *Int. J. Heat Mass Transfer*, 54, pp. 34-42, 2011.
- [21] K. Vafai and L. Zhu, Analysis of two-layered micro-channel heat sink concept in electronic cooling, *Int. J. Heat Mass Transfer*, 42, pp. 2287-2297, 1997.